
THEORETICAL ANALYSIS OF RESONANCE STATES IN ${}^4\text{H}$, ${}^4\text{He}$, AND ${}^4\text{Li}$ ABOVE THREE-CLUSTER THRESHOLD

V. VASILEVSKY^{1,2}, F. ARICKX², J. BROECKHOVE², V.N. ROMANOV¹

UDC 539.142
© 2004

¹Bogolyubov Institute for Theoretical Physics, Nat. Acad. Sci. of Ukraine
(Kyiv, Ukraine),

¹²Departement Wiskunde en Informatica, Universiteit Antwerpen (RUCA)
(Antwerpen, Belgium)

The resonance states of ${}^4\text{H}$, ${}^4\text{He}$, and ${}^4\text{Li}$ embedded in the three-cluster $d + N + N$ continuum are investigated within a three-cluster model. The model treats the Pauli principle exactly and incorporates the Faddeev components for a proper description of the boundary conditions for the two- and three-body continua. The hyperspherical harmonics are used to distinguish and enumerate channels of the three-cluster continuum. It is shown that the effective barrier created by the three-cluster configuration $d + N + N$ is strong enough to accommodate two resonance states.

The theoretical study of the “ground states” of ${}^4\text{H}$ and ${}^4\text{Li}$ and the excited states of all three nuclei was carried out mainly through resonance state analysis. Of all resonances, the first excited 0^+ state has received most attention. In none of the descriptions, the role of three-cluster channels was properly considered, and so resonance states induced by this channel could not be theoretically discovered and analyzed.

Introduction

In this paper, we study the nature of resonance states in ${}^4\text{H}$, ${}^4\text{He}$, and ${}^4\text{Li}$. All these nuclei have a rich structure of resonance states [1]. There are 4 well-determined resonances in ${}^4\text{H}$ and ${}^4\text{Li}$, and up to 15 resonance states were detected in ${}^4\text{He}$. Most of these resonances have a width that is much larger than the resonance energy when measured from the lowest threshold. Although these resonances have been experimentally confirmed, they can hardly be observed in current theoretical model descriptions of these systems through standard elastic and inelastic scattering quantities such as S -matrix elements, differential or total cross sections, and so on.

For many years, the four-nucleon system was studied by different microscopic and semi-microscopic methods. Different forms of the Schrödinger equation (differential [2, 3], integral [4–6], integro-differential [7–9], matrix or algebraic [11–13], ... ones) have been used to study these nuclei. Special attention was paid to ${}^4\text{He}$, the only nuclear 4-particle system featuring a bound state.

Our objective is to determine the type and nature of resonance states in ${}^4\text{H}$, ${}^4\text{He}$ and ${}^4\text{Li}$ that are reproduced within a three-cluster microscopic model. For all three nuclei, we will consider one single three-cluster configuration $d + N + N$. This is certainly the most dominant three-cluster channel, as it has the lowest energy threshold. Moreover, one can easily construct all binary channels for these nuclei within such a description. In ${}^4\text{He}$ for example, this configuration allows one to study resonances created by the two-cluster channels $p+{}^3\text{H}$, $n+{}^3\text{He}$, and $d + d$, as well as by the three-cluster channel $d + p + n$. The latter should be very important, because 7 resonance states were detected above the $d+p+n$ threshold. It is interesting to note in the same context that all four resonance states of ${}^4\text{H}$ lie below the three-cluster $d+n+n$ threshold, whereas two resonances in ${}^4\text{Li}$ are found above the $d + p + p$ threshold.

We propose a modification of the method formulated in [14–16] and used in [17, 18] to study resonances embedded in the three-cluster continuum and reactions with three-cluster exit channels. The method was shown to provide a suitable instrument for investigating

Borromian nuclei (for instance, ${}^6\text{He}$) and nuclei with prominent three-cluster features (like ${}^6\text{Be}$). We wish to extend the method proposed in [14, 16] to handle systems, in which binary channels play a prominent role, by including the correct boundary conditions for both binary and ternary channels. The results obtained in [14, 19] and in [17, 18] allow us to restrict the model space to the most relevant subspace.

To reach this objective, we have to:

- specify the microscopic modelling of the three-cluster configuration and the approximations to be used in calculations,
- construct a set of dynamic equations that take into account the proper boundary conditions for both binary and ternary channels,
- implement reliable numerical methods to calculate continuous spectrum wave functions and S -matrix elements.

1. Model and Methodology

We propose the following trial wave function for the 4-particle systems

$$\Psi = \Psi_1 + \Psi_2 + \Psi_3 = \mathcal{A}\{\Phi_1(A_1)\Phi_2(A_2)\Phi_3(A_3) \times [f_1(\mathbf{x}_1, \mathbf{q}_1) + f_2(\mathbf{x}_2, \mathbf{q}_2) + f_3(\mathbf{x}_3, \mathbf{q}_3)]\}, \quad (1)$$

where $\Phi_\alpha(A_\alpha)$ is the antisymmetric and translationally invariant internal wave function of the A_α nucleon system, and $\mathbf{x}_\alpha, \mathbf{q}_\alpha$ are the familiar Jacobi coordinates denoting the relative position of two of the clusters (\mathbf{x}_α) and the relative position of the third cluster with respect to the former two-cluster subsystem (\mathbf{q}_α):

$$\mathbf{x}_\alpha = \sqrt{\frac{A_\beta A_\gamma}{A_\beta + A_\gamma}} \left[\frac{\sum_{j \in A_\beta} \mathbf{r}_j}{A_\beta} - \frac{\sum_{k \in A_\gamma} \mathbf{r}_k}{A_\gamma} \right],$$

$$\mathbf{q}_\alpha = \sqrt{\frac{A_\alpha (A_\beta + A_\gamma)}{A_\alpha + A_\beta + A_\gamma}} \times \left[\frac{\sum_{i \in A_\alpha} \mathbf{r}_i}{A_\alpha} - \frac{\sum_{j \in A_\beta} \mathbf{r}_j + \sum_{k \in A_\gamma} \mathbf{r}_k}{A_\beta + A_\gamma} \right],$$

with (α, β, γ) being cyclic permutations of $(1, 2, 3)$. The three components of the wave functions $\{\Psi_1, \Psi_2, \Psi_3\}$ (more precisely $\{f_1, f_2, f_3\}$) have to be determined by solving the many-particle Schrödinger equation. Specific symmetries of the system can reduce the number of components: if the three-cluster configuration contains two identical clusters, only two distinguishable

components $\{f_1, f_2\}$ will occur; this is the case for ${}^4\text{H}$ and ${}^4\text{Li}$. If all three clusters are identical (impossible for the 4-particle system though), only one independent component $\{f_1\}$ would occur.

We shall use a matrix or algebraic form of the Schrödinger equation. To this end, we expand the wave function $f_\alpha(\mathbf{x}_\alpha, \mathbf{q}_\alpha)$ in an oscillator basis (referred to as a BiOscillator (BO) basis):

$$f_\alpha(\mathbf{x}_\alpha, \mathbf{q}_\alpha) = \sum_{n_y, l, n_x, \lambda} C_{n_y, l, n_x, \lambda}^{(\alpha)} |n_y, l, n_x, \lambda; LM\rangle_\alpha, \quad (2)$$

where

$$|n_y, l, n_x, \lambda; LM\rangle_\alpha = \Phi_{n_y, l}(q_\alpha) \Phi_{n_x, \lambda}(x_\alpha) \{Y_l(\hat{\mathbf{q}}_\alpha) \cdot Y_\lambda(\hat{\mathbf{x}}_\alpha)\}_{LM} \quad (3)$$

and $\Phi_{n, l}(q)$ is the familiar (radial) oscillator function:

$$\Phi_{n, l}(q) = (-1)^n \sqrt{\frac{2\Gamma(n+1)}{\Gamma(n+l+3/2)}} \frac{1}{b^{3/2}} \left(\frac{q}{b}\right)^l \times \exp\left\{-\frac{1}{2}\left(\frac{q}{b}\right)^2\right\} L_n^{l+1/2}\left(\left(\frac{q}{b}\right)^2\right). \quad (4)$$

The total angular momentum L of the three s -clusters is a vector sum of two partial angular momenta l_α and λ_α associated with the respective Jacobi coordinates \mathbf{x}_α and \mathbf{q}_α .

As each cluster function $\Phi_\alpha(A_\alpha)$ is antisymmetric by construction, the antisymmetrization operator in (1) only involves the permutation of nucleons between clusters, and it can be represented as

$$\hat{\mathcal{A}} = 1 + \hat{\mathcal{A}}_{12} + \hat{\mathcal{A}}_{23} + \hat{\mathcal{A}}_{31} + \hat{\mathcal{A}}_{123}, \quad (5)$$

where $\hat{\mathcal{A}}_{\alpha\beta}$ exchanges nucleons from clusters α and β , and $\hat{\mathcal{A}}_{123}$ permutes particles from all three clusters. In some respects, this antisymmetrization operator is similar to a short range interaction. Indeed, the antisymmetrization is noticeable only when the distance between clusters is small. At larger distances, both the potential energy and the antisymmetrization effects become negligibly small. The operator $\hat{\mathcal{A}}_{123}$ is important only when the distance between all three clusters is less than a certain restricted value. If one of the clusters (say, cluster α) is far away from the two other clusters β and γ , and the latter are close to one other, $\hat{\mathcal{A}}_{\beta\gamma}$ will have a pronounced contribution, as well as the two-cluster interaction $\hat{V}_{\beta\gamma}$ derived from the NN -potential.

Each set of Jacobi coordinates \mathbf{x}_α and \mathbf{q}_α and each set of oscillator functions (3)

$$\{|n_y, l_\alpha, n_x, \lambda_\alpha; LM\rangle_\alpha\} \quad (6)$$

for $\alpha = 1, 2$ or 3 cover the whole configuration space (i.e., account for all possible relative positions of three clusters in space). We will limit ourselves to the subspace $\{|n_y, l_\alpha = L, n_x, \lambda_\alpha = 0; LM\rangle\}$ of the total Hilbert space. Two arguments for such a choice can be given (in particular for the 4-particle system):

1. We deal with s -shell clusters, and the two-cluster compound subsystems also are s -shell nuclei; the latter (d , ${}^3\text{H}$ and ${}^3\text{He}$) have a ground state containing a dominant S -wave contribution.
2. It was shown in [14, 15, 19] that this subspace dominates the full Hilbert space. For instance, the ground state energy of ${}^6\text{He}$ and ${}^8\text{He}$ obtained within this subspace differs by less than 1% from the energy obtained in the full Hilbert space. It was also shown that this subspace dominates the wave function of the 2^+ state of ${}^6\text{He}$, appearing as a resonance embedded in the three-cluster continuum $\alpha + n + n$, as well.

To include the proper boundary conditions, we will split the oscillator space $\{C_{n_y, l, n_x, \lambda}^{(\alpha)}\}$ ($\alpha = 1, 2, 3$) into the internal and asymptotic parts. The former consists of the basis functions of the lowest N_i oscillator shells (i.e. all functions with $N = n_y + n_x = 0, 1, 2, \dots, N_i$; it involves $(N_i + 1)(N_i + 2)/2$ basis functions for each value of α). With this size of the internal region in oscillator space, one can evaluate the maximal size of the three-cluster system in the coordinate space by using the correspondence between the oscillator and coordinate representations (see details in [20, 21])

$$R_{\max} \simeq b\sqrt{4N_i + 6}. \quad (7)$$

If, for instance, the oscillator length $b = 1.5$ fm and $N_i = 15$, then $R_{\max} \simeq 12$ fm. The maximal distance between any pair of clusters will be of the same magnitude. R_{\max} also corresponds to the minimal size of the three-cluster system in the asymptotic region. So all three clusters are close to one another in the internal region, which means that all antisymmetrization components are important, as well as all interactions between clusters.

In the asymptotic region, we distinguish two different regimes. In the first regime, the distance between two clusters is small, while the third one is far apart. In the

second regime, all three clusters are well separated. If a selected pair of clusters (say, β and γ clusters) has (a) bound state(s), then the first regime is responsible for the scattering of the third cluster by the compound $\beta + \gamma$ subsystem. This process can be described by two-body asymptotics. The second regime is associated with the full disintegration of the three-cluster system into three independent (non-interacting) clusters. These two regimes have to be treated differently. This means that two different forms of the wave function have to be used to properly describe these processes. It will require some reconstruction of the basis functions in order to suit both two- and three-body physical processes in the exit channels.

In the first regime of the asymptotics, we can neglect all antisymmetrization components but $\hat{A}_{\beta\gamma}$. As for the potential energy, the most important contribution is generated by the two-cluster potential $\hat{V}_{\beta\gamma}$. The other components $\hat{V}_{\alpha\beta}$ and $\hat{V}_{\alpha\gamma}$, originating from the short-range NN -forces, are negligibly small, and only long-range Coulomb forces are of importance. The wave function in the coordinate and oscillator representations can then be factorized as

$$\begin{aligned} \Psi_\alpha &= \hat{A} \{ \Phi_1(A_1) \Phi_2(A_2) \Phi_3(A_3) f_\alpha(\mathbf{x}_\alpha, \mathbf{q}_\alpha) \} \simeq \\ &\simeq \hat{A}_{\beta\gamma} \{ \Phi_\beta(A_\beta) \Phi_\gamma(A_\gamma) g_\alpha(\mathbf{x}_\alpha) \} \Phi_\alpha(A_\alpha) f_\alpha^{(a)}(\mathbf{q}_\alpha) = \\ &= \Psi_\alpha^{(2)} \cdot \Phi_\alpha(A_\alpha) f_\alpha^{(a)}(\mathbf{q}_\alpha) = \\ &= \sum_{n_y, l, n_x, \lambda} C_{n_y, l, n_x, \lambda}^{(\alpha)} |n_y, l, n_x, \lambda; LM\rangle_\alpha = \\ &= \sum_{n_x, \lambda} \sum_{n_y, l} C_{n_x, \lambda}^{(\alpha)} \cdot C_{n_y, l}^{(\alpha)} |n_y, l, n_x, \lambda; LM\rangle_\alpha. \end{aligned}$$

The two-cluster wave function $\Psi_\alpha^{(2)}$ (its counterpart in the oscillator space is $\{C_{n_x, \lambda}^{(\alpha)}\}$) is an eigenfunction of the two-cluster Hamiltonian (8)

$$\hat{H}_\alpha^{(2)} = \sum_{i \in A_\beta + A_\gamma} \hat{T}_i + \sum_{i < j \in A_\beta + A_\gamma} \hat{V}(ij). \quad (8)$$

By solving the Schrödinger equation

$$\sum_{\tilde{n}_x=0}^{N_2} \langle n_x, \lambda | \hat{H}_\alpha^{(2)} - E^{(\alpha)} | \tilde{n}_x, \lambda \rangle C_{\tilde{n}_x, \lambda}^{(\alpha)} = 0 \quad (9)$$

with a chosen number of basis functions N_2 , we obtain the bound state(s) $E_\sigma^{(\alpha)}$ ($\sigma = 0, 1, \dots$) of the two-cluster subsystem, which determine the threshold energy of the two-body break up of the three-cluster system.

In the second regime of the asymptotics we can neglect the antisymmetrization operator and the short-range components of the inter-cluster potential. In this regime, we use the Hyperspherical Harmonics (HH) basis to describe the full decay of the three-cluster system, because (see, for instance, [14, 17, 22, 23]) this basis is the obvious choice for such a type of the three-cluster behavior. The transition from the bioscillator basis $|n_y, l, n_x, \lambda; LM\rangle_\alpha$ to the HH basis $|n_\rho, K; l, \lambda; LM\rangle_\alpha$ (see details of the definition of HH functions in, e.g., [16]) is performed by an orthogonal matrix. This transformation can be calculated in a straightforward way.

The asymptotic part of the wave function will then be represented by two sets of expansion coefficients

$$\left\{ C_{n_y, L}^{(\alpha, E_0^{(\alpha)})}; C_{n_\rho, K_{\min}; L}^{(\alpha)}, C_{n_\rho, K_{\min}+2; L}, \dots, C_{n_\rho, K_{\max}; L}^{(\alpha)} \right\}, \quad (10)$$

where $K_{\min} = L$. All expansion coefficients in the asymptotic region have a similar form and consist of incoming ($\psi_L^{(+)}$, $\psi_K^{(+)}$) and outgoing ($\psi_L^{(-)}$, $\psi_K^{(-)}$) waves (see details of the definition in [17, 18]):

$$C_{n_y, L}^{(\alpha, E_0^{(\alpha)})} \simeq \sqrt{2R_{n_y}} \left[\delta_{c_0; \alpha} \psi_L^{(-)}(k_\alpha R_{n_y}) - S_{c_0; \alpha} \psi_L^{(+)}(k_\alpha R_{n_y}) \right], \quad (11)$$

$$C_{n_\rho, K; L}^{(\alpha)} \simeq (2\rho_n)^2 \left[\delta_{c_0; \alpha K} \psi_K^{(-)}(k\rho_n) - S_{c_0; \alpha K} \psi_K^{(+)}(k\rho_n) \right], \quad (12)$$

where the index c_0 denotes the entrance channel and

$$k = \sqrt{\frac{2m}{\hbar^2} E}, \quad \rho_n = b\sqrt{4n_\rho + 2K + 6}; \quad (13)$$

$$k_\alpha = \sqrt{\frac{2m}{\hbar^2} (E - E_0^{(\alpha)})}, \quad R_{n_y} = b\sqrt{4n_y + 2L + 3}. \quad (14)$$

Note that the index α enumerates the binary channels, while both indices α and K distinguish the ternary channels. Thus, c_0 equals α_0 , if the entrance channel is a binary one, or $c_0 = \alpha_0, K_0$ for the three-cluster entrance channel.

With this definition of the asymptotic part of the wave function, we deduce the equations for the

scattering parameters and wave function. By taking into account (9)–(12), we obtain

$$\begin{aligned} & \sum_{\bar{\alpha}} \sum_{\tilde{n}_y, \tilde{n}_x \leq N_i} \alpha \langle n_y, n_x | \hat{H} - E | \tilde{n}_y, \tilde{n}_x \rangle_{\bar{\alpha}} C_{\tilde{n}_y, \tilde{n}_x}^{(\bar{\alpha})} - \\ & - \sum_{\bar{\alpha}} S_{c_0; \bar{\alpha}} \sum_{\tilde{n}_y > N_i} \alpha \langle n_y, n_x | \hat{H} - E | \tilde{n}_y, E_0^{(\bar{\alpha})} \rangle_{\bar{\alpha}} \times \\ & \times \psi_L^{(+)}(k_{\bar{\alpha}} R_{\tilde{n}_y}) - \sum_{\bar{\alpha}} S_{c_0; \bar{\alpha} \tilde{K}} \sum_{\tilde{n}_\rho > N_i} \alpha \langle n_y, n_x | \hat{H} - \\ & - E | \tilde{n}_\rho, \tilde{K} \rangle_{\bar{\alpha}} \psi_{\tilde{K}}^{(+)}(k\tilde{\rho}) = \\ & = - \sum_{\bar{\alpha}} \delta_{c_0; \bar{\alpha}} \sum_{\tilde{n}_y > N_i} \alpha \langle n_y, n_x | \hat{H} - E | \tilde{n}_y, E_0^{(\bar{\alpha})} \rangle_{\bar{\alpha}} \times \\ & \times \psi_L^{(-)}(k_{\bar{\alpha}} R_{\tilde{n}_y}) - \sum_{\bar{\alpha}} \delta_{c_0; \bar{\alpha} \tilde{K}} \sum_{\tilde{n}_\rho > N_i} \alpha \langle n_y, n_x | \hat{H} - \\ & - E | \tilde{n}_\rho, \tilde{K} \rangle_{\bar{\alpha}} \psi_{\tilde{K}}^{(-)}(k\tilde{\rho}). \end{aligned} \quad (15)$$

In the general case of three different clusters, this system of linear equations contains

$$\frac{3}{2} (N_i + 1) (N_i + 2) + 3 + 3N_{\text{ch.HH}} \quad (16)$$

parameters to be determined. Here,

$$N_{\text{ch.HH}} = (K_{\max} - K_{\min}) / 2 + 1 \quad (17)$$

is the number of HH channels. From this total amount, $\frac{3}{2} (N_i + 1) (N_i + 2)$ coefficients represent the wave function in the internal region, and the other $3 + 3N_{\text{ch.HH}}$ parameters determine the elastic and inelastic processes leading to two or three clusters in the exit channels. These parameters unambiguously define the wave functions in the asymptotic region.

2. Results

We use the Minnesota (MP) [24], and the modified Hasegawa–Nagata (MHNP) [25, 26] nucleon-nucleon (NN) potentials. The oscillator radius b is chosen to optimize the bound state energy of a deuteron and equals $b = 1.512$ fm for MP and $b = 1.668$ fm for MHNP. Considering these two potentials reveals the effect of peculiarities of NN -forces on the parameters of resonance states.

In the first calculation, we neglect all binary channels, and only consider the three-cluster channels.

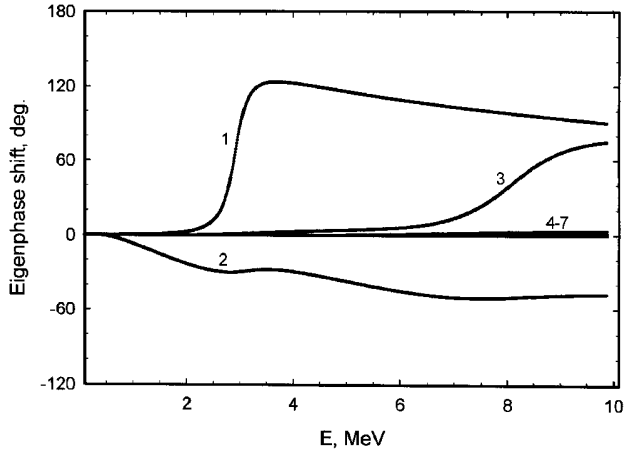


Fig. 1. Eigenphase shifts for the $L^\pi = 1, S = 1$ state of ${}^4\text{Li}$ obtained with the Minnesota potential and $K_{\max} = 11$. The eigenchannels are enumerated

This allows us to understand what kinds of resonances are generated by this channel only. We have omitted spin-orbital components of the NN -forces to reduce the computational burden.

The results obtained in this approximation can be considered to represent a “lower limit” for the width of a resonance, as additional channels will open new decay possibilities of the resonance, which will increase its width. In this respect, the three-cluster approximation will indicate whether some resonance state(s) could survive if binary channels are included.

By solving the dynamic equations (15) for N_c channels, we directly obtain the $N_c \times N_c$ S -matrix. There are two different parametrizations for the S -matrix. In the first one, each element S_{ij} can be represented by the

Table 1. Resonance states of ${}^4\text{H}$, ${}^4\text{He}$, and ${}^4\text{Li}$ created by the three-cluster channel $d + N + N$. Results are obtained with the Minnesota potential

Nucleus	L^π	S	K_{\max}	E_r , MeV	Γ_r , MeV	E_r , MeV	Γ_r , MeV
${}^4\text{H}$	1^-	0	11	1.642	0.367	6.726	2.759
${}^4\text{H}$	1^-	1	11	1.911	0.374	6.958	2.982
${}^4\text{Li}$	1^-	0	11	2.604	0.413	7.787	3.141
${}^4\text{Li}$	1^-	1	11	2.912	0.465	8.085	3.384
${}^4\text{He}$	2^+	0	10	1.950	0.233	2.904	0.207

Table 2. Resonance states of ${}^4\text{H}$, ${}^4\text{He}$, and ${}^4\text{Li}$ created by the three-cluster channel $d + N + N$. Results are obtained with the MHN potential

Nucleus	L^π	S	K_{\max}	E_r , MeV	Γ_r , MeV	E_r , MeV	Γ_r , MeV
${}^4\text{H}$	1^-	0	11	3.972	1.170	9.469	3.440
${}^4\text{H}$	1^-	1	11	3.738	0.950	9.250	3.362
${}^4\text{Li}$	1^-	0	11	0.748	0.093	5.009	1.531
${}^4\text{Li}$	1^-	1	11	0.662	0.056	4.772	1.329
${}^4\text{He}$	2^+	0	10	0.890	0.005	2.436	0.167

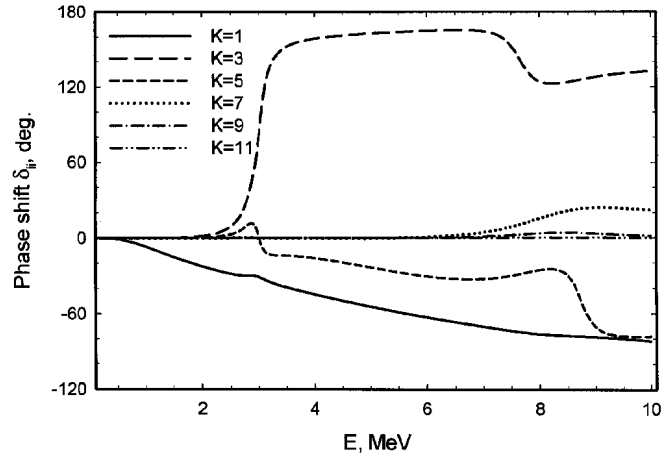


Fig. 2. Phase shifts of the $3 \Rightarrow 3$ scattering for the $L^\pi = 1^-, S = 1$ state of ${}^4\text{Li}$. Results are obtained with the Minnesota potential and $K_{\max} = 11$

phase shift δ_{ij} and the inelastic parameter η_{ij} : $S_{ij} = \eta_{ij} \exp\{2i\delta_{ij}\}$. In the second parametrization, the S -matrix is reduced to a diagonal form by the orthogonal transformation

$$\|S\| = \|O\|^T \cdot \|S^{(E)}\| \cdot \|O\|. \quad (18)$$

The latter procedure leads to N_c uncoupled elastic “eigenchannels”, whose (eigen)phase shifts parametrize the diagonalized $S^{(E)}$ -matrix. We use the eigenphase shifts to determine both the energy and width of the resonances. They are obtained from the following equations:

$$\left. \frac{d^2 \delta_\nu}{d^2 E} \right|_{E=E_r} = 0, \quad \Gamma = 2 \left(\frac{dE}{d\delta_\nu} \right) \Big|_{E=E_r}. \quad (19)$$

We start our analysis from the eigenphase shift. In Fig. 1, we display the eigenphase shift of the so-called $3 \Rightarrow 3$ scattering for $L^\pi = 1^-, S = 1$ state in ${}^4\text{Li}$, obtained with the Minnesota potential. Similar pictures are obtained for other nuclei and different (L^π, S) states and also with the MHN potential. One can see from Fig. 1 that there are two resonance states in ${}^4\text{Li}$, first resonance is narrow and manifests itself through the first eigenchannel, while the second resonance is very broad and appears in the third eigenchannel.

In Figs. 2 and 3, we display the phase shifts δ_{ii} and inelastic parameters η_{ii} connected with the diagonal matrix elements of the original S -matrix. They are obtained for ${}^4\text{Li}$ and with MP. One notices that only two hyperspherical harmonics are responsible for the lowest 1^- resonance state. The $K = 3$ phase shift displays the

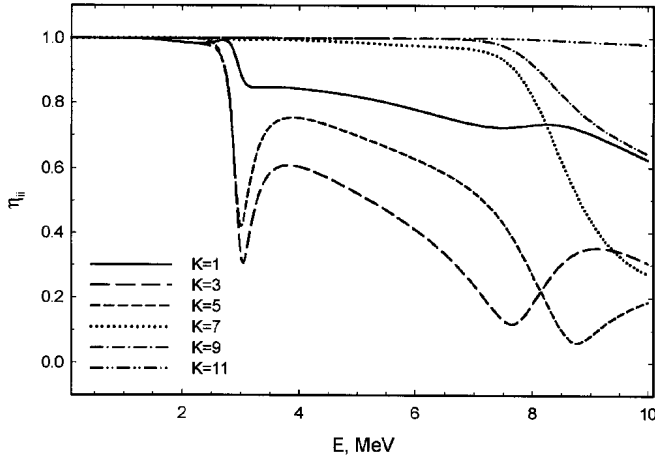


Fig. 3. Inelastic parameters of the $3 \Rightarrow 3$ scattering for the $L^\pi = 1^-$, $S = 1$ state in ${}^4\text{Li}$. Results are obtained with the Minnesota potential and $K_{\text{max}} = 11$

classical behavior for a resonance state, while the $K = 5$ phase shift indicates a “shadow” resonance. Many more hyperspherical momenta are involved in creating the second resonance.

In Tables 1 and 2, we collect the parameters of the resonance states lying above the three-cluster threshold $d + N + N$. The even parity states are obtained with $K_{\text{max}} = 10$, and the odd parity states with $K_{\text{max}} = 11$.

It is known that there is an effective barrier in each channel of a three-cluster system. The barrier is created by a potential well resulted from the NN -interaction between nucleons from different clusters and a centrifugal barrier which is proportional to

$$\frac{\hbar^2}{2m} \frac{K(K+4)}{\rho^2}. \quad (20)$$

In ${}^4\text{He}$ and ${}^4\text{Li}$, the Coulomb repulsion

$$\frac{Z_{\text{eff}}}{\rho} \quad (21)$$

has to be added to the effective barrier. The effective charge Z_{eff} depends on the quantum numbers α , K , l_1 , and l_2 , and its definition can be found in [16]. The deeper the potential well, the larger is the effective barrier and, consequently, more resonance states can be created by such effective barrier. One can see that the effective barrier generated by the MHN potential is deeper than the one connected with the Minnesota potential. As a result of this difference, the resonance states in ${}^4\text{H}$ obtained with the MHN potential have a larger energy than the resonances calculated with the Minnesota potential.

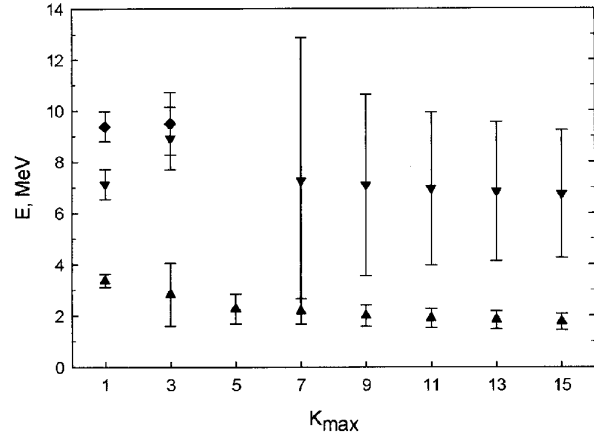


Fig. 4. Energy of the 1^- resonance state of ${}^4\text{H}$ (total spin $S = 1$) as a function of K_{max} . Error bars indicate the double of the resonance width. The calculations have been performed with the Minnesota potential

The results presented in Tables 1 and 2 are obtained for the even parity states with $K_{\text{max}} = 10$ and for the odd parity states with $K_{\text{max}} = 11$. These values for K_{max} are sufficient to obtain stable results. This is demonstrated in Fig. 4, where the parameters (energy and width) of the 1^- resonance in ${}^4\text{H}$ are displayed as functions of K_{max} . The results in Fig. 4 are presented for the Minnesota potential, and similar results are obtained for the MHN potential. We indicate some “false” resonances appearing at small values of K_{max} due to the restriction on decay channels compatible with this K_{max} . When we increase the number of open channels, the “false” resonances disappear and the physical resonances converge to their correct positions.

There are some arguments that the physical resonances do not depend on the boundary conditions implemented or on the used approximations. One can study, e.g., the behavior of the so-called Harris states, i.e. the eigenvalues of the Hamiltonian as a function of the number of basis functions involved in a calculation. It was shown (see, for instance, [27, 28]) that the eigenvalues $E_\nu(n)$ [$E_\nu(n)$ is the ν -th eigenvalue obtained with n basis functions] create plateaus at the energies of resonance states. For a very narrow resonance, this plateau is already observed for a small value of n . For wider resonances, one needs more basis functions to reach a plateau. For a small number of basis functions a wider resonance can become apparent as the repulsion of two eigenvalues (the avoided crossing of two eigenvalues). Such a behavior of these eigenvalues was observed for the Hamiltonian of the three-cluster configuration $d + N + N$ in ${}^4\text{H}$, ${}^4\text{He}$ and ${}^4\text{Li}$.

Conclusion

A microscopic model is formulated to treat properly the two- and three-body boundary conditions. For this aim, the Faddeev component is used. The hyperspherical harmonics are used to enumerate three-cluster channels. They are very valuable for describing the three-cluster asymptotics. Two NN -potentials are involved in the calculations in order to evaluate the sensitivity of the final results with respect to this important factor of the microscopic model.

The model is applied in studying the resonance states in ${}^4\text{H}$, ${}^4\text{He}$, and ${}^4\text{Li}$ nuclei created by the three-cluster configuration $d + N + N$. The results presented here demonstrate that the three-cluster configuration creates an effective centrifugal barrier which allows one to accommodate several resonances. The effect of two-cluster channels on the position and width of three-cluster resonances will be discussed in a future work.

One of the authors (V. V.) gratefully acknowledges the University of Antwerp (RUCA) for a “RAFO-gastprofessoraat 2002-2003” and the kind hospitality of the members of the research group “Computational Modeling and Programing” of the Department of Mathematics and Computer Sciences, University of Antwerp, RUCA, Belgium.

1. *Tilley D. R., Weller H. R., Hale G. M.*//Nucl. Phys. A.— 1992.— **541**. — P.1.
2. *Viviani M., Kievsky A., Rosati S. et al.*//Phys. Rev. Lett.— 2001.— **86**.— P.3739.
3. *Viviani M.*//Nucl. Phys. A.— 2001.— **689**.— P.308.
4. *Filikhin I. N., Yakovlev S. L.*//Yad. Fiz. (Phys. Atomic Nuclei).— 2000.— **63**.— P.79(69).
5. *Carbonell J.*//Nucl. Phys. A.— 2001.— **684**.— P.218–226.
6. *Carbonell J.*//Few Body Syst. Suppl.— 2000.— **12**.— P.439–444.
7. *Kaneko T., Tang Y. C.*//Progr. Theor. Phys.— 2002.— **107**.— P.833.
8. *Pfizinger B., Hofmann H. M., Hale G. M.*//Phys. Rev. C.— 2001.— **64**.— P.044003.
9. *Kanada H., Kaneko T., Tang Y. C.*//Ibid.— 1991.— **43**.— P.371–378.
10. *Kaneko T., Tang Y. C.*//Progr. Theor. Phys.— 2002.— **107**.— P.833–837.
11. *Vasilevsky V. S., Kovalenko T. P., Filippov G. F.*//Yad. Fiz.— 1988.— **48**.— P.217–223(346–357).
12. *Vasilevsky V. S., Rybkin I. Yu., Filippov G. F.*//Ibid.— 1990.— **51**.— P.71–77(112–123).
13. *Hofmann M., Hale G. M.*//Nucl. Phys. A.— 1997.— **613**.— P.69.
14. *Vasilevsky V. S., Nesterov A. V., Arickx F., Leuven P. V.*//Phys. Atomic Nucl.— 1997.— **60**.— P. 343–349.
15. *Arickx F., Leuven P. V., Vasilevsky V., Nesterov A.* //Proc. 5th. Intern. Spring Seminar in Nuclear Physics.—Singapore: World Scientific, 1995.
16. *Vasilevsky V. S., Nesterov A. V., Arickx F., Broeckhove J.*//Phys. Rev. C.— 2001.— **63**.— P. 034606.
17. *Vasilevsky V. S., Nesterov A. V., Arickx F., Broeckhove J.*//Ibid.— 2001.— **63**.— P. 034607.
18. *Vasilevsky V. S., Nesterov A. V., Arickx F., Broeckhove J.*//Ibid.— P.064604.
19. *Vasilevsky V. S., Nesterov A. V., Chernov O.*//Phys. Atom. Nucl. (Yad. Fiz.)— 2001.— **64**, N8.— P.1409–1415(1486–1492).
20. *Filippov G. F., Okhrimenko I. P.*//Sov. J. Nucl. Phys.— 1981.— **32**.— P. 480.
21. *Filippov G. F.*//Ibid.— 1981.— **33**.— P. 488.
22. *Danilin B.V., Zhukov M.V.*//Yad. Fiz. (Phys. Atomic Nuclei).— 1993.— **56**.— P. 67 (460).
23. *Cobis A., Fedorov D. V., Jensen A. S.*//Phys. Rev. C.— 1998.— **58**.— P.1403–1421.
24. *Thompson D. R., LeMere M., Tang Y. C.*//Nucl. Phys. A.— 1977.— **268**.— P. 53–66.
25. *Hasegawa A., Nagata S.*//Progr. Theor. Phys.— 1971.— **45**.— P.1786–1807.
26. *Tanabe F., Tohsaki A., Tamagaki R.*//Ibid.— 1975.— **53**.— P.677–691.
27. *Filippov G. F., Vasilevsky V. S., Chopovsky L. L.*//Sov. J. of Particles and Nuclei (Elem. Chast. Atom. Yadra).— 1985.— **16**.— P.153–177(349–406).
28. *Ho Y. K.*//Phys. Repts.— 1993.— **99**.— P. 1–68.

Received 09.12.03

ТЕОРЕТИЧНИЙ АНАЛІЗ РЕЗОНАНСНИХ СТАНІВ В ${}^4\text{H}$, ${}^4\text{He}$ ТА ${}^4\text{Li}$ НАД ТРИКЛАСТЕРНИМ ПОРОГОМ

В.С. Василевський, Ф. Арікс, Я. Брукхов, В.М. Романов

Резюме

У рамках трикластерної моделі досліджено резонансні стани ядер ${}^4\text{H}$, ${}^4\text{He}$ і ${}^4\text{Li}$, занурені в трикластерний континуум $d + N + N$. Ця модель точно враховує принцип Паулі та використовує фаддєєвські компоненти для коректного врахування граничних умов у дво- та тричастинковому континуумі. Канали тричастинкового континуума розрізняються і нумеруються за допомогою гіперсферичних функцій. Показано, що ефективний бар'єр, який породжується трикластерною конфігурацією $d + N + N$, достатньо інтенсивний для створення двох резонансів.